

1

Some nice title

2 Thomas Dobbelaere, Emmanuel Hanert (and other co-authors to be determined)

3

February 9, 2021

4

Abstract

5

Some nice abstract

6

1 Introduction

7

2 Methods

8

2.1 Wind and atmospheric pressure for Hurricane Irma

9

- Reduction of wind speed according to Harper et al. (2010)
- HURDAT 2 (Landsea and Franklin, 2013) for hurricane pressure with radius of maximum wind speed according to Knaff et al. (2018) using Holland pressure profile (Lin and Chavas, 2012).

13

2.2 Hydrodynamic model

Ocean currents generated during hurricane Irma in the Florida Reef Tract (FRT) were modelled using the unstructured-mesh depth-integrated coast ocean model SLIM¹. The model mesh covers an area similar to the model extent of Dobbelaere et al. (2020), that includes the FRT but also the Florida Strait and part of the Gulf of Mexico (Figure 1). However, this area has been slightly extended northeastward and westward in order to include the location of buoys for wave outputs validation. Furthermore, in order to

¹<https://www.slim-ocean.be>

withstand potential cell drying due to storm conditions in this study, we used the conservative mode of SLIM with wetting-drying, whose equations write:

$$\begin{aligned} \frac{\partial H}{\partial t} + \nabla \cdot (\mathbf{U}) &= 0 \\ \frac{\partial \mathbf{U}}{\partial t} + \nabla \cdot \left(\frac{\mathbf{U}\mathbf{U}}{H} \right) &= -f\mathbf{e}_z \times \mathbf{U} + \alpha g H \nabla(H - h) - \frac{1}{\rho} \nabla p_{\text{atm}} + \frac{1}{\rho} \boldsymbol{\tau}_s \quad (1) \\ &\quad + \nabla \cdot (\nu \nabla \mathbf{U}) - \frac{C_b}{H^2} |\mathbf{U}| \mathbf{U} + \gamma(\mathbf{U}_* - \mathbf{U}) \end{aligned}$$

where H is the water column height and \mathbf{U} is the depth-averaged transport; f is the Coriolis coefficient; g is the gravitational acceleration; h is the bathymetry; α is a coefficient stating whether the mesh element is wet ($\alpha = 1$) or dry ($\alpha = 0$); ν is the viscosity; C_b is the bottom drag coefficient; ∇p_{atm} is the atmospheric pressure gradient; $\boldsymbol{\tau}_s$ is the surface stress due to wind; and γ is a relaxation coefficient towards a reference transport \mathbf{U}_* . As in Frys et al. (2020) and Dobbelaere et al. (2020), SLIM currents were relaxed towards HYCOM (Chassignet et al., 2007) in regions where the water depth exceeds a given threshold. At very high wind speeds, the white cap is blown off the crest of the waves, which generates a layer of droplets that acts as a slip layer for the winds at the ocean-atmosphere interface (Holthuijsen et al., 2012). This causes a saturation of the wind drag coefficient for strong winds (Donelan et al., 2004; Powell et al., 2003). To account for the impact of this saturation on the surface wind stress in our model, we implemented the wind drag parameterization of Moon et al. (2007).

The mesh resolution depended only on the distance to coastlines and reefs, bathymetry and bathymetry gradient in order to satisfy SWAN refinement criterion $h/A \geq a$, where h is the water depth and A is the element area. The mesh was generated using the Python library seamsh², based on the open-source mesh generator GMSH (Geuzaine and Remacle, 2009) and is composed of approximately 7.7×10^5 elements. The coarsest elements, far away from the FRT, had a characteristic length size of about 5 km. Figure 1 depicts how a 100-m spatial resolution mesh simulated fine-scale details of the ocean currents and significant wave height generated by hurricane Irma in the Florida Keys.

²<https://pypi.org/project/seamsh/>

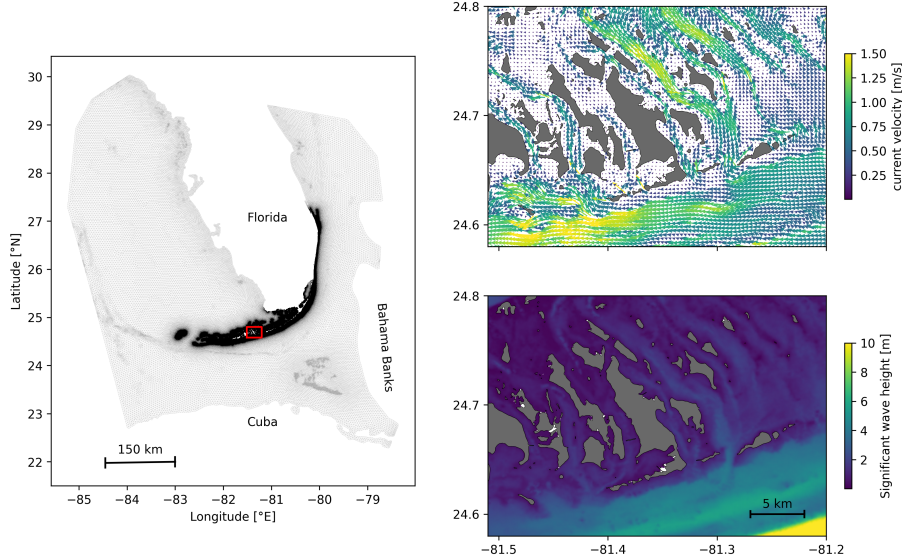


Fig. 1: Mesh of the computational domain with snapshots of simulated instantaneous currents and significant wave height on 2017-09-10 at 11:00:00. The mesh resolution ranges from 100 m in the Florida Keys to a maximum of 5 km offshore.

39 2.3 Wave model

Waves were modelled using the parallel unstructured SWAN (Booij et al., 1999)

$$\frac{\partial N}{\partial t} + \nabla_{\mathbf{x}} \cdot [(\mathbf{c}_g + \mathbf{u})N] + \frac{\partial}{\partial \theta}[c_\theta N] + \frac{\partial}{\partial \sigma}[c_\sigma N] = \frac{S_{in} + S_{ds} + S_{nl}}{\sigma} \quad (2)$$

- 40 • Exponential growth by wind by Janssen (1991)
- 41 • Whitecapping formulation by Komen et al. (1984)
- 42 • Bottom dissipation according to Madsen et al. (1989)
- 43 • Same mesh as SLIM
- 44 • For wave boundary conditions, spectra from WW3 (Tolman et al., 2009)

45 2.4 Coupled model

- 46 Express z_0 for Madsen bottom friction from Manning dissipation used in
- 47 SLIM obtained following the methodology of Dietrich et al. (2011)

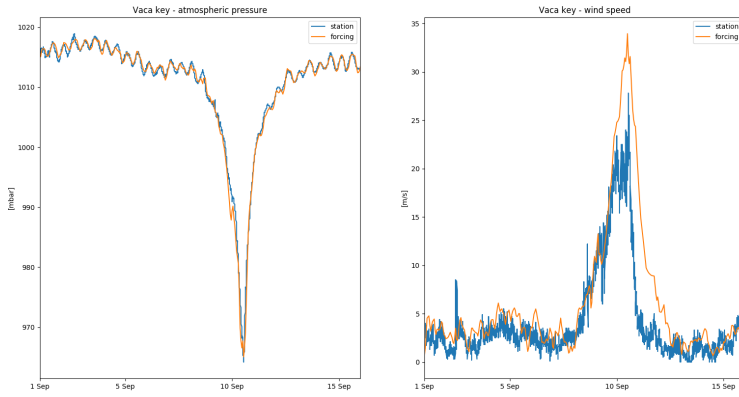


Fig. 2: The atmospheric forcings have been validated with meteorological station observations at Vaca Key. The reconstructed atmospheric pressure and wind speed agree well with field measurements.

48 3 Results

49 3.1 Validation

50 3.2 Impact of waves

51 4 Discussion and conclusions

52 Impact of waves on coral connectivity

53 Ability of wave model to correctly capture gradient in significant wave height
54 due to current-waves interactions under tropical cyclones depends on:

- 55 • Spatial (10km → 5km) and spectral (36 dir. → 48 dir.) resolution
56 (Hegermiller et al., 2019)
- 57 • Directional spreading of incident waves (Villas Bôas et al., 2020)

58 Conflict of Interest Statement

59 The authors declare that the research was conducted in the absence of any
60 commercial or financial relationships that could be construed as a potential

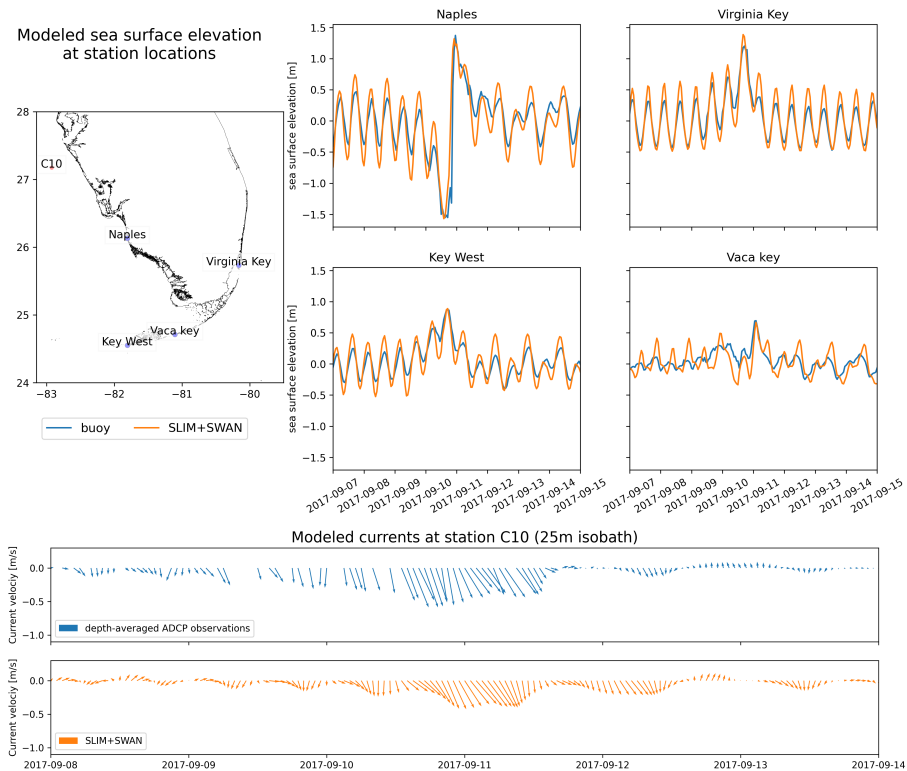


Fig. 3: The sea-surface elevation produced by the coupled wave-current model agrees with SSE and current velocity observations at different stations. The fit is particularly good in the Florida Keys and in Naples, on the inner Florida shelf. The coupled model currents have been validated against current meter data on the inner Florida shelf. The current speed and direction during the hurricane agrees well with the observations.

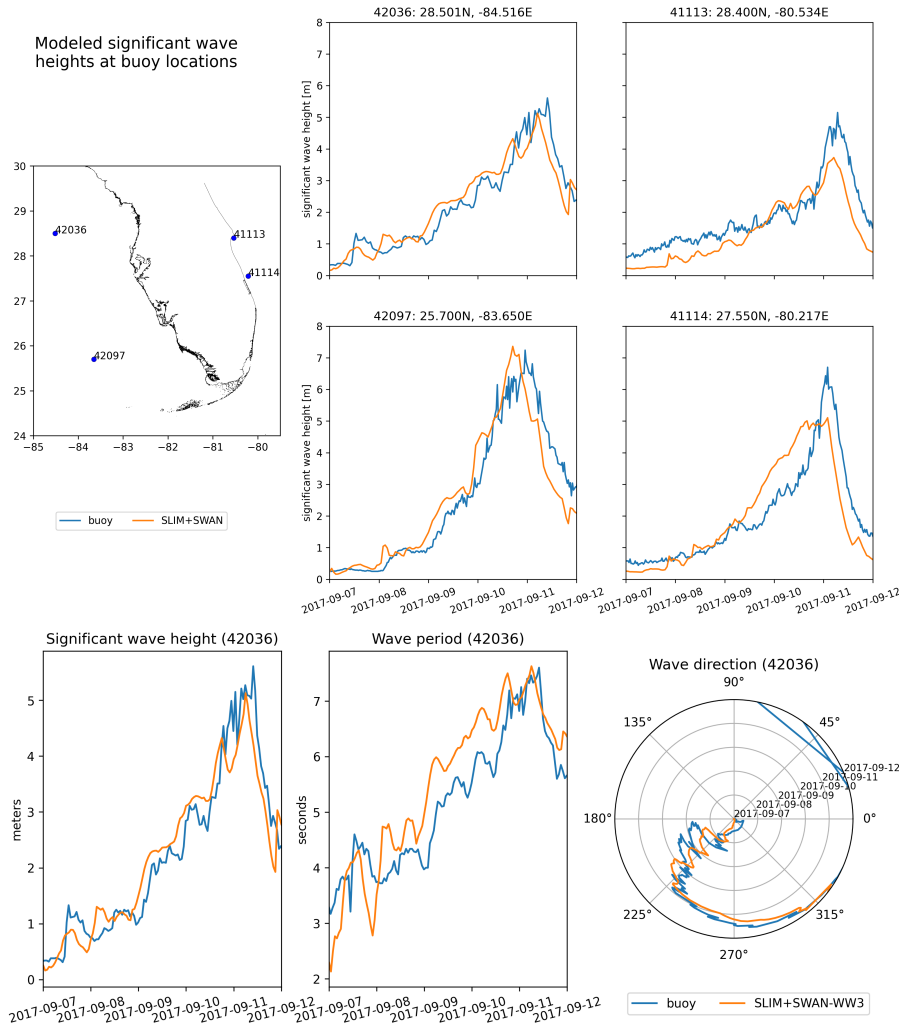


Fig. 4: The significant wave height produced by the coupled model has been compared to buoy measurements at 4 different stations. The timing and amplitude of the peak during the hurricane is correctly reproduced for all stations. For station 42036, the period and direction of the waves also agree well with observations

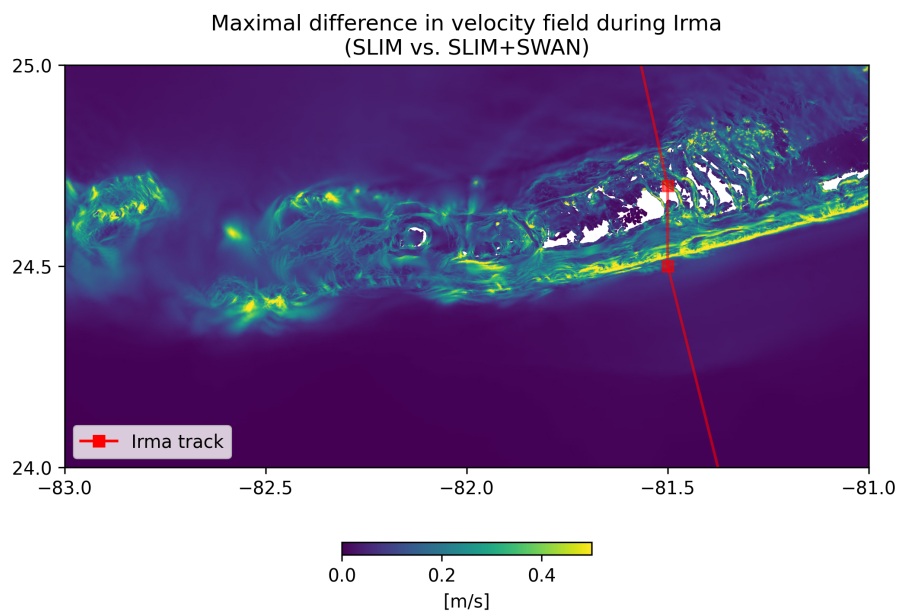


Fig. 5: Maximum of the difference between SLIM and SLIM+SWAN currents speed between 2017-09-07 00:00:00 and 2017-09-13 00:00:00. The difference between the coupled and uncoupled model, which represents the effect of the wave-induced stress, can yield differences of 0.5 m/s in the simulated currents during the passage of the hurricane. SLIM+SWAN currents velocities are larger than the currents modeled by SLIM alone.

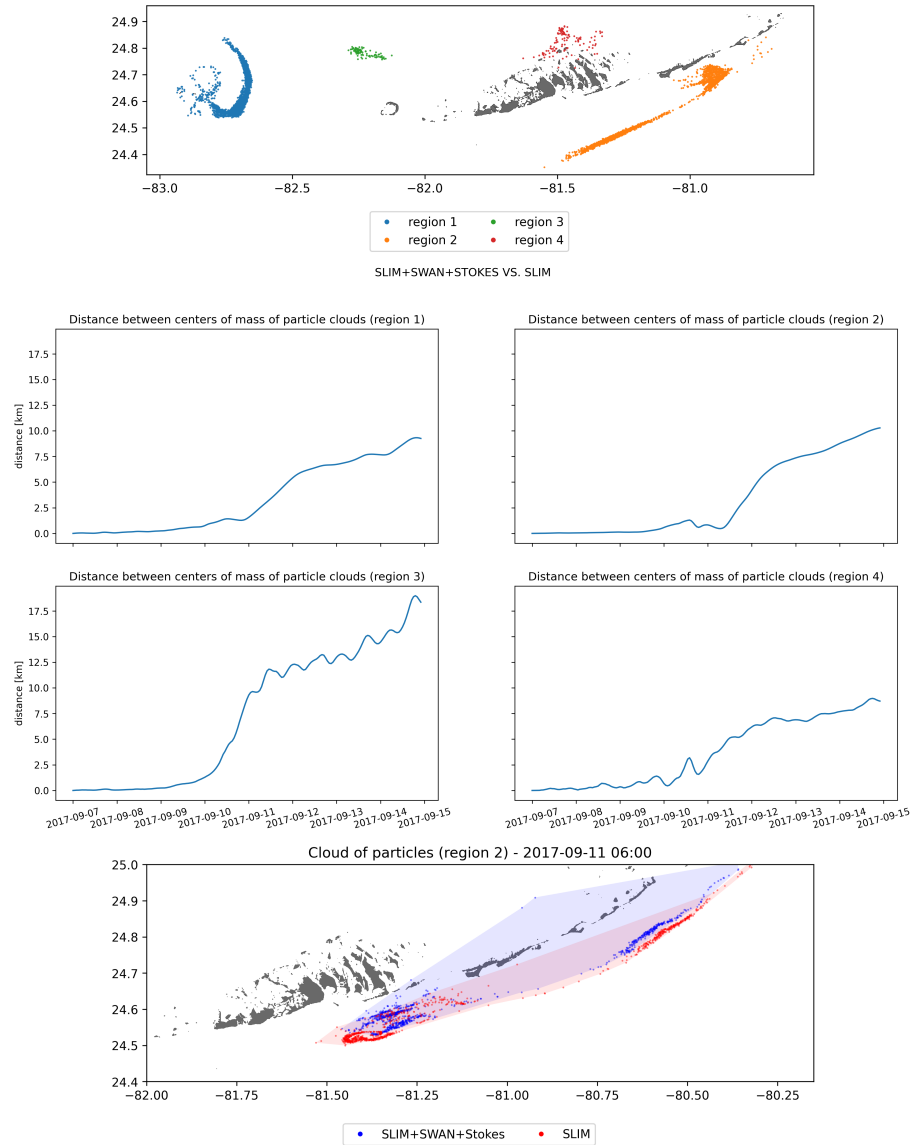


Fig. 6: Comparison of passive drifters trajectories with SLIM+SWAN+Stokes drift vs. SLIM alone. A snapshot of the positions of the particles released from region 2 is shown after the passage of Irma in the Florida Keys. Particles advected by the currents of the coupled model tend to remain on the shelf while particles advected by SLIM alone are mostly transported along the shelf break

⁶¹ conflict of interest.

⁶² Author Contributions

⁶³ Funding

⁶⁴ Acknowledgments

⁶⁵ Computational resources were provided by the Consortium des Équipements
⁶⁶ de Calcul Intensif (CÉCI), funded by the F.R.S.-FNRS under Grant No. 2.5020.11.
⁶⁷ Thomas Dobbelaere is a PhD student supported by the Fund for Research
⁶⁸ training in Industry and Agriculture (FRIA/FNRS).

⁶⁹ Supplementary Material

⁷⁰ The Supplementary Material for this article is attached to the submitted
⁷¹ document.

⁷² References

- ⁷³ Booij, N., Ris, R. C., and Holthuijsen, L. H. (1999). A third-generation wave
⁷⁴ model for coastal regions: 1. Model description and validation. *Journal*
⁷⁵ *of geophysical research: Oceans*, 104(C4):7649–7666.
- ⁷⁶ Chassignet, E. P., Hurlbert, H. E., Smedstad, O. M., Halliwell, G. R., Hogan,
⁷⁷ P. J., Wallcraft, A. J., Baraille, R., and Bleck, R. (2007). The HYCOM
⁷⁸ (hybrid coordinate ocean model) data assimilative system. *Journal of*
⁷⁹ *Marine Systems*, 65(1-4):60–83.
- ⁸⁰ Dietrich, J., Westerink, J., Kennedy, A., Smith, J., Jensen, R., Zijlema, M.,
⁸¹ Holthuijsen, L., Dawson, C., Luettich, R., Powell, M., et al. (2011).
⁸² Hurricane gustav (2008) waves and storm surge: Hindcast, synoptic
⁸³ analysis, and validation in southern Louisiana. *Monthly Weather Review*,
⁸⁴ 139(8):2488–2522.

- 85 Dobbelaere, T., Muller, E. M., Gramer, L. J., Holstein, D. M., and Hanert, E.
86 (2020). Coupled epidemic-hydrodynamic modeling to understand the
87 spread of a deadly coral disease in Florida. *Frontiers in Marine Science*,
88 7:1016.
- 89 Donelan, M., Haus, B., Reul, N., Plant, W., Stiassnie, M., Gruber, H., Brown,
90 O., and Saltzman, E. (2004). On the limiting aerodynamic roughness of
91 the ocean in very strong winds. *Geophysical Research Letters*, 31(18).
- 92 Frys, C., Saint-Amand, A., Le Hénaff, M., Figueiredo, J., Kuba, A., Walker, B.,
93 Lambrechts, J., Vallaeyns, V., Vincent, D., and Hanert, E. (2020). Fine-
94 scale coral connectivity pathways in the Florida Reef Tract: implications
95 for conservation and restoration. *Frontiers in Marine Science*, 7:312.
- 96 Geuzaine, C. and Remacle, J.-F. (2009). Gmsh: A 3-d finite element mesh
97 generator with built-in pre-and post-processing facilities. *International
98 journal for numerical methods in engineering*, 79(11):1309–1331.
- 99 Harper, B., Kepert, J., and Ginger, J. (2010). *Guidelines for converting
100 between various wind averaging periods in tropical cyclone conditions*.
101 Citeseer.
- 102 Hegermiller, C. A., Warner, J. C., Olabarrieta, M., and Sherwood, C. R.
103 (2019). Wave-current interaction between Hurricane Matthew wave
104 fields and the Gulf Stream. *Journal of Physical Oceanography*,
105 49(11):2883–2900.
- 106 Holthuijsen, L. H., Powell, M. D., and Pietrzak, J. D. (2012). Wind and waves
107 in extreme hurricanes. *Journal of Geophysical Research: Oceans*,
108 117(C9).
- 109 Janssen, P. A. (1991). Quasi-linear theory of wind-wave generation applied
110 to wave forecasting. *Journal of physical oceanography*, 21(11):1631–
111 1642.
- 112 Knaff, J. A., Sampson, C. R., and Musgrave, K. D. (2018). Statistical tropi-
113 cal cyclone wind radii prediction using climatology and persistence:
114 Updates for the western North Pacific. *Weather and Forecasting*,
115 33(4):1093–1098.

- 116 Komen, G., Hasselmann, S., and Hasselmann, K. (1984). On the exis-
117 tence of a fully developed wind-sea spectrum. *Journal of physical*
118 *oceanography*, 14(8):1271–1285.
- 119 Landsea, C. W. and Franklin, J. L. (2013). Atlantic hurricane database un-
120 certainty and presentation of a new database format. *Monthly Weather*
121 *Review*, 141(10):3576–3592.
- 122 Lin, N. and Chavas, D. (2012). On hurricane parametric wind and appli-
123 cations in storm surge modeling. *Journal of Geophysical Research: Atmospheres*, 117(D9).
- 125 Madsen, O. S., Poon, Y.-K., and Graber, H. C. (1989). Spectral wave
126 attenuation by bottom friction: Theory. In *Coastal Engineering 1988*,
127 pages 492–504.
- 128 Moon, I.-J., Ginis, I., Hara, T., and Thomas, B. (2007). A physics-based
129 parameterization of air–sea momentum flux at high wind speeds and
130 its impact on hurricane intensity predictions. *Monthly weather review*,
131 135(8):2869–2878.
- 132 Powell, M. D., Vickery, P. J., and Reinhold, T. A. (2003). Reduced drag coeffi-
133 cient for high wind speeds in tropical cyclones. *Nature*, 422(6929):279–
134 283.
- 135 Tolman, H. L. et al. (2009). User manual and system documentation of
136 WAVEWATCH III TM version 3.14. *Technical note, MMAB Contribution*,
137 276:220.
- 138 Villas Bôas, A. B., Cornuelle, B. D., Mazloff, M. R., Gille, S. T., and Arduin,
139 F. (2020). Wave–current interactions at meso-and submesoscales:
140 Insights from idealized numerical simulations. *Journal of Physical*
141 *Oceanography*, 50(12):3483–3500.